

## Path-integral Monte Carlo calculation of the effects of thermal disorder in extended x-ray-absorption fine structure of copper

S. a Beccara and P. Fornasini

*Dipartimento di Fisica, Università di Trento, Via Sommarive 14, I-38050 Povo (Trento), Italy*

(Received 6 February 2008; revised manuscript received 28 March 2008; published 30 May 2008)

The distributions of interatomic distances of the first four coordination shells of copper and their leading cumulants have been determined by a path-integral Monte Carlo calculation on a many-body potential model, in the temperature range of 4–300 K. The asymmetry of the distance distribution, measured by the third cumulant, is much larger for the first shell than for the outer shells. The mean value of the distance between neighboring atoms is given for each shell by the first cumulant of the distribution. This allowed us to test a well-known method of estimating the thermal expansion of each shell from the second and third cumulants of its distribution. This method gave values smaller by 40% for the first shell and much smaller for all outer shells.

DOI: [10.1103/PhysRevB.77.172304](https://doi.org/10.1103/PhysRevB.77.172304)

PACS number(s): 63.20.–e, 61.05.cj, 02.70.Uu, 65.40.De

One of the most interesting applications of extended x-ray-absorption fine structure (EXAFS) spectroscopy<sup>1</sup> is the investigation of local structural and dynamical properties of crystals, which are different from the average properties probed by diffraction techniques. It has recently been shown that one can experimentally detect the difference between the thermal expansions of the interatomic distances measured by EXAFS and by Bragg diffraction.<sup>2,3</sup> From this difference, original information can be obtained on local lattice dynamics, useful to study phase transitions and the origin of negative thermal expansion in some classes of crystalline structures.<sup>4,5</sup> These findings once again stress the relevance of a deeper understanding of the effects of atomic thermal motion on EXAFS spectra.<sup>1</sup> In this regard, a still controversial issue concerns the relation between the thermal expansion of interatomic distances and the asymmetry of the corresponding distributions.<sup>3,6</sup>

An EXAFS experiment samples a one-dimensional distribution of distances, which is the sum of the contributions of the different single-scattering (SS) and multiple-scattering (MS) paths originating from and terminating at the absorber atom. SS paths correspond to the coordination shells. For moderate disorder, the distribution of distances of each path can be parameterized in terms of its leading cumulants, the first three cumulants representing the average value, variance, and asymmetry of the distribution.<sup>3,7</sup> The connection between second cumulant and *parallel* mean square relative displacement (MSRD) in SS paths was established quite early.<sup>8</sup> More recently, the experimental detection of the difference between EXAFS and diffraction thermal expansions has led to the evaluation of the SS *perpendicular* MSRD.<sup>2</sup>

No general agreement has been reached as yet on the relation between thermal expansion, measured by the first cumulant, and asymmetry of the distribution of interatomic distances, measured by the third cumulant. For two-atomic molecules, the EXAFS cumulants can actually be expressed as a function of the force constants of the one-dimensional interaction potential,<sup>9,10</sup> and the knowledge of the second and third cumulants is sufficient to recover the thermal expansion. For many-atomic systems, the EXAFS cumulants can be connected by the same analytical relations to the force

constants of a one-dimensional effective pair potential.<sup>11</sup> While some authors believe that the thermal expansion can be evaluated from the second and third cumulants even in many-atomic systems,<sup>6,9</sup> others claim that a rigid shift of the distance distribution can add a significant contribution to the thermal expansion.<sup>3,12,13</sup> The controversy is related to the connection between the crystal potential and the resulting thermodynamic properties, on one hand, and the effective pair potentials corresponding to the distance distributions of different coordination shells, on the other hand.

A method for calculating EXAFS cumulants from the force constants of the crystal potential, based on first principles perturbation theory, was proposed by Fujikawa and Miyanaga<sup>14</sup> and mainly applied to one-dimensional systems,<sup>15</sup> although some attempts have been done also for fcc crystals.<sup>16</sup> Promising results on three-dimensional systems have been obtained by path-integral techniques, based on the use of effective potentials<sup>17</sup> or on Monte Carlo sampling.<sup>18</sup> A widespread phenomenological approach consists in approximating the thermal behavior of each scattering path by an anharmonic one-dimensional Einstein model<sup>9,10</sup> and in expressing the EXAFS cumulants as a function of the force constants of the effective anharmonic Einstein potential. The first-shell effective pair potential of copper has been evaluated by Hung and Rehr<sup>19</sup> in terms of the Morse interaction potential, and more recently by Vila *et al.*<sup>6</sup> from *ab initio* calculations.

Accurate experiments on simple systems, such as copper and germanium, have shown that the temperature dependences of both second and third cumulants of the first coordination shell are in good agreement with the behavior expected for a constant-shape effective potential within the framework of a statistical quantum perturbation approach.<sup>2,3</sup> The thermal variation of the first cumulant seems, however, to depend, for the first shell, not only on the asymmetry of the distribution but also on the shift of its maximum when the temperature is varied, corresponding to a rigid shift of the effective pair potential.

Additional information could in principle be obtained from the study of farther coordination shells. However, the extension of an accurate cumulant analysis of experimental

data beyond the first shell has been up to now severely limited by MS effects, which require an exceedingly large number of parameters to be fitted to experimental data. As a matter of fact, in a recent study of copper, extended up to the fourth shell, while the parallel MSRDs of the outer shells could be singled out, no reliable information could be obtained on the thermal expansion and third cumulant of each one of the outer shells.<sup>3</sup>

Numerical simulation techniques give the possibility of extending our understanding beyond the limits of experiment. Classical Monte Carlo simulations of solid krypton<sup>20,21</sup> suggest that the outer shells are much less asymmetric than the first one and the increase in the first cumulant nearly corresponds for the outer shells to the shift of the maximum position of the distribution. The behavior of a van der Waals solid like krypton can however hardly be generalized to other crystals.

Path-integral Monte Carlo<sup>22</sup> (PIMC) is particularly appealing for reproducing EXAFS parameters since it takes into account both anharmonicity and low-temperature quantum effects. Basically, PIMC consists in sampling the thermal density matrix after it has been transformed into the convolution of  $P$  matrices—each one with effective temperature  $P$  times higher—corresponding to  $P$  copies of the system, linked together by a harmonic potential. The set of atomic configurations sampled from the thermal density matrix can be exploited to calculate observable physical quantities by means of configurational averages. PIMC is essentially an exact method in the limit  $P \rightarrow \infty$ , the reliability of the results depending only on the validity of the Born–Oppenheimer approximation and on the quality of the interatomic potential used to model the crystal potential. In a previous work,<sup>18</sup> the effectiveness of PIMC was verified by reproducing the cumulants of the first shell of copper.

In this work, PIMC calculations have been done on a larger simulation box, of  $4 \times 4 \times 4$  conventional unit cells (256 atoms) with periodic boundary conditions; as a consequence, the analysis of configurations could be safely extended up to the fourth shell. The cell parameter was adjusted at each temperature according to available crystallographic data.<sup>23</sup> A set of temperatures ranging from 4 to 300 K was explored. A many-body potential of the tight-binding family in second-moment approximation (SMA-TB)<sup>24</sup> was chosen. The total energy is a sum over all atoms  $i$  of a many-body attractive term,

$$E_b^i = - \left[ \sum_{j \neq i} \xi^2 e^{-2q(r_{ij}/r_0 - 1)} \right]^{1/2}, \quad (1)$$

and a two-body Born–Mayer repulsive term,

$$E_r^i = A \sum_{j > i} e^{-p(r_{ij}/r_0 - 1)}. \quad (2)$$

The potential has already been tested by Cleri and Rosato<sup>24</sup> and by Bryan Edwards *et al.*;<sup>25</sup> in both cases, the parameters  $A$ ,  $\xi$ ,  $p$ , and  $q$  were fitted to experimental values of cohesive energy, lattice parameter, and elastic constants. A good reproduction of phonon dispersion curves and atomic mean square displacements (MSDs) was obtained by Cleri and Rosato.<sup>24</sup> Edwards *et al.*<sup>25</sup> calculated the high temperature EXAFS cu-

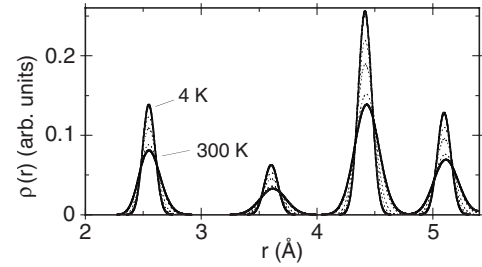


FIG. 1. Radial distribution functions calculated at all considered temperatures from 4 to 300 K.

mulants of copper by molecular dynamics simulations. In Ref. 18, the relevance of a many-body term such as Eq. (1) for reproducing the third EXAFS cumulant was stressed, by comparison to a simple pair potential.

The distributions of interatomic distances of the first four shells, calculated from the configurations generated by PIMC (Fig. 1), can be neatly singled out at all the considered temperatures. For each shell, the first three cumulants  $C_i^*$  ( $i=1,2,3$ ) have been calculated as  $\langle r \rangle$ ,  $\langle (r - \langle r \rangle)^2 \rangle$ , and  $\langle (r - \langle r \rangle)^3 \rangle$  and the mode of the distribution,  $r_{\max}$ , has been evaluated by a polynomial fit around the maximum position. Additionally, the parallel and perpendicular MSRDs,  $\langle \Delta u_{\parallel}^2 \rangle$  and  $\langle \Delta u_{\perp}^2 \rangle$ , respectively, have been calculated by projecting the atomic displacements from the equilibrium positions along the interatomic distance and within the perpendicular plane, respectively.

The relative bond expansions  $\delta C_1^*/C_1^*$  measured by the first EXAFS cumulants are shown in Fig. 2, left panel, and compared with the experimental values for the first shell<sup>3</sup> and with the relative expansion  $\delta a/a$  of the lattice parameter.<sup>23</sup> Here,  $\delta C_1^* = C_1^*(T) - C_1^*(4 \text{ K})$  and  $\delta a = a(T) - a(4 \text{ K})$ . The difference between the average distance measured by EXAFS,  $\langle r \rangle = |\langle \mathbf{r}_2 - \mathbf{r}_1 \rangle|$ , and the distance between average positions,  $R_c = |\langle \mathbf{r}_2 \rangle - \langle \mathbf{r}_1 \rangle|$ , is due to the effect of vibrations perpendicular to the bond directions, according to<sup>3</sup>

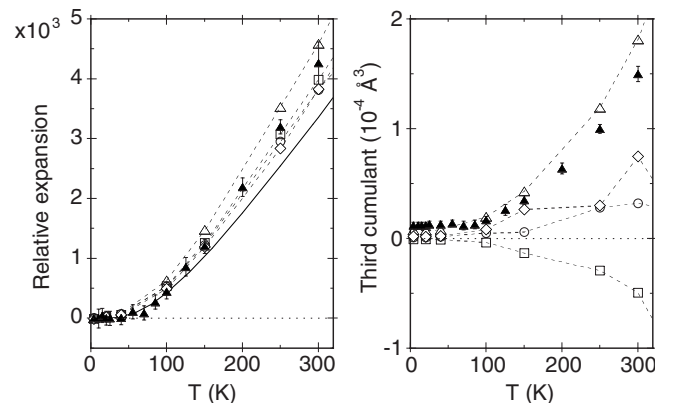


FIG. 2. Relative bond expansions  $\delta C_1^*/C_1^*$  (left panel) and third cumulants (right panel) calculated by PIMC for the first (open triangles), second (squares), third (circles), and fourth (diamonds) coordination shells; the dashed lines are guides to eye. The solid triangles are the first-shell experimental results from Ref. 3. The solid line is the relative expansion  $\Delta a/a$  of the lattice parameter (Ref. 23).

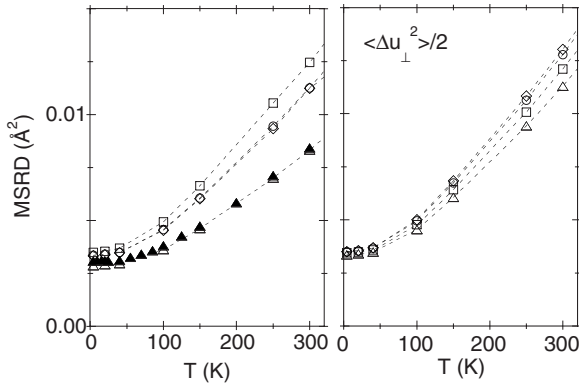


FIG. 3. Parallel MSRDS  $\langle \Delta u_{\parallel}^2 \rangle$  (left panel) and perpendicular MSRDS divided by two,  $\langle \Delta u_{\perp}^2 \rangle / 2$ , for the first (triangles), second (squares), third (circles), and fourth (diamonds) coordination shells. The dashed lines are guides to eye. The solid triangles are the experimental first-shell parallel MSRDS from Ref. 3.

$$\langle r \rangle = R_c + \langle \Delta u_{\perp}^2 \rangle / 2R_c. \quad (3)$$

For each coordination shell, the perpendicular MSRDS  $\langle \Delta u_{\perp}^2 \rangle$  obtained by inverting Eq. (3) are in very good agreement with the values evaluated from the projection of atomic displacements. The parallel MSRDS  $\langle \Delta u_{\parallel}^2 \rangle$ , evaluated from the projection of atomic displacements, are in excellent agreement with the second cumulant. The agreement represents a self-consistency check of PIMC calculations.

Parallel and perpendicular MSRDS are shown in Fig. 3, and the temperatures of the best-fitting correlated Debye models<sup>8,26</sup> are listed in Table I. The Debye temperature is slightly smaller for the second shell than for the other shells, indicating a weaker correlation, in agreement with lattice dynamical calculations for other fcc crystals.<sup>27</sup> The Debye temperatures best fitting the perpendicular MSRDS calculated by PIMC are very similar for the different shells, the exception being now the first shell, where again the smaller value indicates a weaker correlation. The agreement between theory and experiment for the parallel MSRDS can be evaluated by visual inspection for the first shell (Fig. 3) and by comparing the best-fitting Debye temperatures for all the four shells (Table I).

The values of the third cumulants  $C_3^*$  for the first four coordination shells of copper, calculated by PIMC, are shown in Fig. 2, right panel. The values for the first shell are positive and in reasonable agreement with the experimental values in Ref. 3. The third cumulant values of the outer shells, calculated by PIMC, are significantly smaller than those of the first shell, the second shell values being even negative.

The asymmetry of a distribution is measured by the skewness parameter  $\beta = C_3^* / (C_2^*)^{3/2}$ . The values of  $\beta$  at 300 K are listed in Table I. The first-shell distribution is much more asymmetric than the distributions of the outer shells because it is characterized by a larger third cumulant and a smaller second cumulant. Actually, the effective pair potential does not correspond to the bare pair potential; it results from a thermal average of all the interactions, for a given shell, within the crystal, and one can reasonably expect that this

TABLE I. Debye temperatures best fitting the experimental (Ref. 3) and calculated parallel MSRDS  $\theta_{\parallel}$  and the calculated perpendicular MSRDS  $\theta_{\perp}$ . Skewness parameters  $\beta = C_3^* / (C_2^*)^{3/2}$  at 300 K.

Shell		First	Second	Third	Fourth
$\theta_{\parallel}$ (K)	Expt.	328.5	291.0	322.5	322.0
	PIMC	324.2	291.6	316.4	320.9
$\theta_{\perp}$ (K)	PIMC	276.7	296.9	295.4	295.6
$\beta$ (at 300 K)	PIMC	0.24	-0.03	0.03	0.06

effect is different for different coordination shells. An approximate calculation for fcc crystals, based on interatomic Morse potentials, has recently shown that the first-shell effective pair potential is less anharmonic than the bare Morse potential;<sup>19,28</sup> the present results suggest that the anharmonicity is still weaker for the effective pair potentials of the outer shells.

The different behaviors found for the third cumulants of different coordination shells stimulate a deeper investigation of their relation with thermal expansion. The thermal expansion of the average interatomic distance  $\langle r \rangle$  is measured by the temperature variation  $\delta C_1^*$  of the first EXAFS cumulant. For a two-atomic system, the thermal expansion is solely due to the anharmonicity of the pair potential, i.e., to the asymmetry of the distribution, and can be indifferently evaluated from the first cumulant as  $\delta C_1^*$ , or from the second and third cumulants, within the first order quantum perturbation approximation, as  $b = -3k_3 C_2^* / k_{\parallel}$  (Ref. 9, where  $a$  corresponds to our  $b$ ). For a crystal, the effective EXAFS pair potential can be temperature dependent, and the bond thermal expansion  $\delta C_1^*$  can also depend on a shift of the minimum of the effective pair potential, corresponding to a shift of the maximum of the distribution of distances.

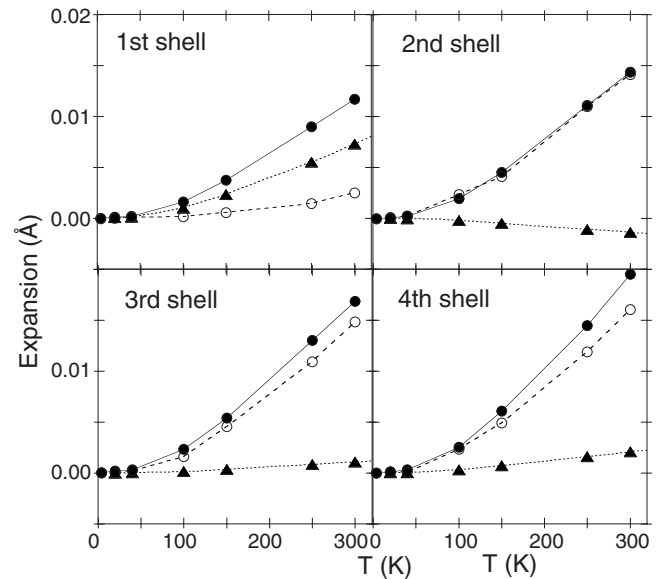


FIG. 4. Comparison between the thermal expansions measured by the first EXAFS cumulants (solid circles), the shifts of the maximum of the distributions of distances (open circles), and the contributions due to the asymmetry of the distributions (triangles).

PIMC results give a powerful insight on this point. In Fig. 4, the temperature dependence  $\delta C_1^* = \delta \langle r \rangle$  of the first cumulant is compared to the shift of the maximum of the distribution (that corresponds to the minimum of the effective pair potential) and with the contribution  $\delta b$  due to the distribution asymmetry for the first four coordination shells. For the first shell, the contribution due to asymmetry prevails and is connected to the relatively high values of the third cumulant; the shift of the maximum of the distribution, however, is not negligible. For the outer shells, the contribution due to asymmetry is much weaker, and the expansion  $\delta C_1^*$  is nearly completely accounted for by the shift of the maximum of the distribution.

In conclusion, the results of PIMC calculations are self-consistent and in agreement with the available experimental data, i.e., first three cumulants of the first shell and the second cumulants of the outer shells. Original information has been obtained on interatomic distances and thermal expansion.

It is clearly shown that the bond thermal expansion depends on both the asymmetry and the shift of the distance distribution, and this dependence is different for different coordination shells. Correspondingly, the temperature dependence of the minimum of the effective pair potential is not negligible and is different for different coordination shells. As a consequence, no simple and general relation can be established between third cumulant and bond thermal expansion. The bond thermal expansion can only be measured by the first cumulant. The third cumulant has to be taken into account in the data analysis to guarantee the accuracy of the first cumulant values; its relevance, however, is smaller for the outer shells than for the first shell.

The authors acknowledge the use of the WIGLAF computer cluster of the Department of Physics of the University of Trento and are grateful to J. J. Rehr, N. Van Hung, A. Sanson, and M. Vaccari for helpful discussions and advice.

- 
- <sup>1</sup>J. Rehr and R. Albers, *Rev. Mod. Phys.* **72**, 621 (2000).  
<sup>2</sup>G. Dalba, P. Fornasini, R. Grisenti, and J. Purans, *Phys. Rev. Lett.* **82**, 4240 (1999).  
<sup>3</sup>P. Fornasini, S. a Beccara, G. Dalba, R. Grisenti, A. Sanson, M. Vaccari, and F. Rocca, *Phys. Rev. B* **70**, 174301 (2004).  
<sup>4</sup>A. Sanson, F. Rocca, G. Dalba, P. Fornasini, R. Grisenti, M. Dapiaggi, and G. Artioli, *Phys. Rev. B* **73**, 214305 (2006).  
<sup>5</sup>M. Vaccari, R. Grisenti, P. Fornasini, F. Rocca, and A. Sanson, *Phys. Rev. B* **75**, 184307 (2007).  
<sup>6</sup>F. D. Vila, J. J. Rehr, H. H. Rossner, and H. J. Krappe, *Phys. Rev. B* **76**, 014301 (2007).  
<sup>7</sup>G. Bunker, *Nucl. Instrum. Methods Phys. Res.* **207**, 437 (1983).  
<sup>8</sup>G. Beni and P. M. Platzman, *Phys. Rev. B* **14**, 1514 (1976).  
<sup>9</sup>A. I. Frenkel and J. J. Rehr, *Phys. Rev. B* **48**, 585 (1993).  
<sup>10</sup>T. Yokoyama, *J. Synchrotron Radiat.* **6**, 323 (1999).  
<sup>11</sup>P. Fornasini, F. Monti, and A. Sanson, *J. Synchrotron Radiat.* **8**, 1214 (2001).  
<sup>12</sup>G. Dalba, P. Fornasini, R. Gotter, and F. Rocca, *Phys. Rev. B* **52**, 149 (1995).  
<sup>13</sup>O. Kamishima, T. Ishii, H. Maeda, and S. Hashino, *Solid State Commun.* **103**, 141 (1997).  
<sup>14</sup>T. Fujikawa and T. Miyanaga, *J. Phys. Soc. Jpn.* **62**, 4108 (1993).  
<sup>15</sup>T. Miyanaga and T. Fujikawa, *J. Phys. Soc. Jpn.* **63**, 1036 (1994).  
<sup>16</sup>H. Katsumata, T. Miyanaga, T. Yokoyama, T. Fujikawa, and T. Ohta, *J. Synchrotron Radiat.* **8**, 226 (2001).  
<sup>17</sup>T. Yokoyama, *Phys. Rev. B* **57**, 3423 (1998).  
<sup>18</sup>S. a Beccara, G. Dalba, P. Fornasini, R. Grisenti, F. Pederiva, A. Sanson, D. Diop, and F. Rocca, *Phys. Rev. B* **68**, 140301(R) (2003).  
<sup>19</sup>N. Van Hung and J. J. Rehr, *Phys. Rev. B* **56**, 43 (1997).  
<sup>20</sup>A. Di Cicco, A. Filipponi, J. P. Itié, and A. Polian, *Phys. Rev. B* **54**, 9086 (1996).  
<sup>21</sup>T. Yokoyama, T. Ohta, and H. Sato, *Phys. Rev. B* **55**, 11320 (1997).  
<sup>22</sup>D. M. Ceperley, *Rev. Mod. Phys.* **67**, 279 (1995).  
<sup>23</sup>Y. S. Touloukian, R. K. Kirby, R. E. Taylor, and P. D. Desai, *Thermophysical Properties of Matter* (Plenum, New York, 1977), Vol. 13.  
<sup>24</sup>F. Cleri and V. Rosato, *Phys. Rev. B* **48**, 22 (1993).  
<sup>25</sup>A. Bryan Edwards, D. J. Tildesley, and N. Binsted, *Mol. Phys.* **91**, 357 (1997).  
<sup>26</sup>M. Vaccari and P. Fornasini, *J. Synchrotron Radiat.* **13**, 321 (2006).  
<sup>27</sup>I. K. Jeong, R. H. Heffner, M. J. Graf, and S. J. L. Billinge, *Phys. Rev. B* **67**, 104301 (2003).  
<sup>28</sup>N. Van Hung and P. Fornasini, *J. Phys. Soc. Jpn.* **76**, 084601 (2007).